Dynamics of Electron Attachment and Ionization Processes in the CCl_4 Molecule: An ab Initio MO and Direct Dynamics Study

Hiroto Tachikawa

Division of Molecular Chemistry, Graduate School of Engineering, Hokkaido University, Sapporo 060, Japan

Received: May 28, 1997; In Final Form: July 23, 1997[⊗]

Electron attachment and ionization processes in the CCl_4 molecule to form CCl_4 radical anion and cation, $CCl_4 + e^-$ (hole) → CCl_4^- (CCl_4^+), have been studied by means of both ab initio MO and direct dynamics calculations. The ab initio calculations of CCl_4^- show that two conformers of the radical anion CCl_4^- are obtained for the stable structures: the elongated and compressed structures distorted from T_d symmetry of neutral CCl_4 due to the Jahn−Teller effect. The elongated structure is more stable by 11.8 kcal/mol relative to the compressed structure at the MP4SDQ/6-31G(d) level. The CCl_4^+ is unstable relative to its dissociation limit (CCl_3^+ and Cl atom). The direct dynamics trajectory calculations show that the radical anion CCl_4^-, formed by a vertical electron attachment of the CCl_4 molecule, leads directly to the elongated form of CCl_4^-. On the other hand, CCl_4^+ formed by a vertical ionization directly dissociates to $CCl_3^+ + Cl$ without an activation barrier. The reaction mechanisms of electron attachment and ionization processes are discussed on the basis of theoretical results.

1. Introduction

Ionic species stabilized in the solid phase at low temperature have been extensively studied from experimental and theoretical points of view.[1] Electron spin resonance (ESR) spectroscopy combined with ab initio MO calculation gives valuable information on the electronic states of the ionic species with unpaired electrons.[2]

Tetrachloromethane, CCl_4, is one of the most popular molecules in radiation chemistry because of its ability to capture electrons and holes. In addition, its ionic species formed in the condensed phase have been extensively studied as a model of halocarbons.[3] A large number of the studies on ESR and pulse- and γ-radiolysis of CCl_4 have been presented. Bonazzola et al. observed an ESR spectrum of CCl_4^- trapped in CCl_4 matrixes at 77 K.[4] They suggested by analyzing g-tensor components that CCl_4^- has a C_{3v} structure and the excess electron is occupied in an σ^* antibonding orbital. In addition, they carried out an ab initio MO calculation of CCl_4^- with a minimal basis set (STO-3G) and suggested that CCl_4^- has a compressed structure in which one of the C−Cl bonds is shortened as a most stable form.

The pulse- and γ-radiolysis studies on ionic species of CCl_4 (CCl_4^+, CCl_4^-, and so on) have been carried out by several groups.[5] The studies mainly focused on the assignment of absorption spectra appearing at visible regions of the ionic species formed by radiolysis. The assignments of the spectra of the ionic species are however still in controversy because of their chemical instability.[5,6] Therefore, the electron attachment and ionization processes in CCl_4 are not clearly understood.

In the present study, the electronic states and structures of the ionic species of CCl_4 molecule are investigated by means of an ab initio MO method. In addition, direct ab initio dynamics calculations are carried out in order to elucidate the electron attachment and ionization processes in CCl_4 molecules (i.e, electron- and hole-capturing processes):

$$CCl_4 + e^- \rightarrow [CCl_4^-]_{unstable} \rightarrow [CCl_4^-]_{relaxed}$$

$$CCl_4 + \text{hole} \rightarrow [CCl_4^+]_{unstable} \rightarrow [CCl_4^+]_{relaxed}$$

where $[X]_{unstable}$ is an unstable complex formed by vertical electron attachment and ionization of CCl_4. The main purposes of this study are (1) to determine theoretically the electronic and geometrical structures of the radical ions CCl_4^- and CCl_4^+ and (2) to elucidate their formation processes theoretically (i.e., the dynamics of the unstable complexes).

The collision cross section of CCl_4 with a beam of electrons and alkali-metal atoms has been measured as gas-phase experiments. According to data from such investigations, the formations of the parent CCl_4^- anion is very sensitive to the nature of the molecular excitations.[7,8] The anions are formed with a relatively low cross section in the electron-transfer collision with a potassium atom beam.[7,8]

As a theoretical point of view, Gutsev investigated the electronic and geometrical structures of the anion radicals CCl_n^- ($n = 1-4$) by means of the local density functional (LDF) method.[9] The calculations implied that the anion CCl_4^- is nonrigid due to the presence of a number of local minima on the potential energy surface. Lunell and co-workers calculated the structure of $CFCl_3^+$, which is very similar to CCl_4^+, by means of the HF/3-21G* method.[2b] They suggested that $CFCl_3^+$ is unstable and spontaneously dissociates to $CFCl_2^+$ and Cl-(atom). Although the structures of ionic species of CCl_4 seem to be understood theoretically, the dynamics is scarcely known. To interpret the results of experimental investigations, it is useful to give theoretical information on dynamics for the electron- and hole-capturing processes in CCl_4.

2. Method of Calculations

Ab initio MO calculations were carried out at the MP4SDQ level of theory with the 6-31G* basis set. Geometries for neutral CCl_4, neutral radical CCl_3, singlet state ion CCl_3^+, and radical

[⊗] Abstract published in *Advance ACS Abstracts,* September 15, 1997.

S1089-5639(97)01715-5 CCC: $14.00

TABLE 1: Optimized Parameters for CCl_4 and CCl_4^- Calculated at the MP4SDQ/6-31G* Level. Bond Length and Angles Are in Angstroms and Degrees. The Values Calculated by the MP2/6- 31+G* Method Are Given in Parentheses

		CCl_4^-		
	CCl_4	compressed	elongated	TS
r_1	1.7756	1.8160	2.4815 (2.4903)	1.9596
r_2	1.7756	1.9852	1.7768 (1.7639)	1.9339
θ	109.46	106.56	108.59 (107.89)	109.89

ions CCl_4^- and CCl_4^+ were fully optimized at the MP4SDQ/6-31G* level. To test the effect of the diffuse function, a 6-31+G* basis set was used for the calculation of CCl_4^-. However, MP2/6-31+G* calculation gave similar results at the MP4SDQ/6-31G* level of theory, as can be clearly seen in Table 1. Hence we will discuss the electronic states by using the results of MP4SDQ/6-31G* calculations.

In general, the classical trajectory is performed on an analytically fitted potential energy surface as previously carried out by us.[10] However, it is not appropriate to predetermine the reaction surfaces of CCl_4^- and CCl_4^+ systems due to the large number of degrees of freedom ($3N$ - 6 = 9, where N is the number of atoms in the reaction system). Therefore, in the present study, we applied the direct MO trajectory calculation with all degrees of freedom.[11]

First, a trajectory calculation of the neutral CCl_4 system was carried out in order to obtain the initial structure of CCl_4^- and CCl_4^+. We used the HF/3-21G* optimized geometry of CCl_4 as an initial structure. At the start of the trajectory calculation, atomic velocities are adjusted to give a temperature of 10 K. All dynamics calculations are performed at the ab initio HF/3-21G* level of theory. By using the configurations randomly selected from the trajectory calculation of CCl_4, the trajectory calculations were carried out for the CCl_4^- and CCl_4^+ systems. The potential energy (total energy) and energy gradient were calculated at each time step. In the calculation of the classical trajectory, we assumed that each atom moves as a classical particle on the HF/3-21G* multidimensional potential energy surface. The equations of motion for n atoms in a molecule are given by

$$m_i \, dv_{\mu i}/dt = F_{\mu i}$$

$$dx_{\mu i}/dt = v_{\mu i}$$

where $x_{\mu i}$ (μ = 1, 2, 3) are the three Cartesian coordinates of the ith atom with mass m_i and $F_{\mu i}$'s are the three components of the force acting on the ith atom. These equations were numerically solved by the Runge−Kutta method. No symmetry restriction was applied to the calculation of the gradients in the Runge−Kutta method. The time step size was chosen by 0.20 fs, and a total of 25 trajectories were run.

3. Results

I. Ab Initio MO Calculations. *A. Radical Anion CCl_4^-.* First, the geometry of the neutral CCl_4 molecule is fully optimized by means of the MP4SDQ/6-31G* calculation. The optimized geometrical parameters are listed in Table 1. The C−Cl distance is calculated to 1.7756 Å, which is in good agreement with an experimental value (1.767 Å).[12]

To obtain the structure of the CCl_4^- radical anion, the geometry optimizations are carried out from several initial structures on the potential energy surface by the energy gradient method. Two stable structures are obtained for CCl_4^-: one is an elongated structure in which one of C−Cl bonds is elongated and the other one is a compressed structure in which one of the C−Cl bonds is shorter than those of the other C−Cl bonds. The structural parameters of the CCl_4^- are summarized in Table 1. For the elongated structure, one of the C−Cl distances is calculated to be 2.4815 Å and the other distances are 1.7768 Å, suggesting that the structure of CCl_4^- is much distorted from that of neutral CCl_4. In the compressed form, the C−Cl distances are calculated to be 1.8160 and 1.9852 Å. The angles from the C_3 axis (θ, ∠Cl−C−Cl) in both structures are very close to the neutral CCl_4 molecule. The elongated structure is more stable by 11.9 kcal/mol than the compressed one. The vertical electron affinity of CCl_4 is calculated to be −27.5 kcal/mol (= −1.19 eV), which is in good agreement with the experimental value of −0.94 eV.[13]

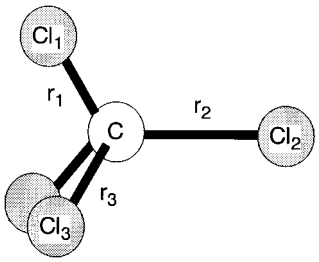

Figure 1. Structure and geometrical parameters of the CCl_4 system.

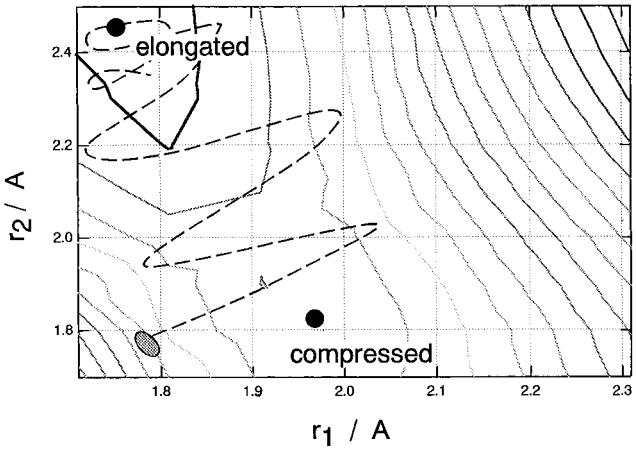

Figure 2. Potential energy surface of the CCl_4^- system calculated at the MP2/6-31G* level. Contours are drawn for each 0.01 au. Dots mean two stable structures of CCl_4^-: the elongated and compressed forms of CCl_4^-. The hatched region indicates the Franck−Condon region of the neutral CCl_4 molecule. The dashed line schematically represents a trajectory starting from the hatched region.

The ab initio calculation also shows that there is an activation barrier between the compressed and elongated structures. The structure of the transition state (TS) is given in Table 1. The C−Cl distances are 1.9596 and 1.9339 Å at the TS. The barrier heights from compressed and elongated structures are calculated to be 0.4 and 12.2 kcal/mol, respectively. This result implies that the compressed structure is unstable on the CCl_4^- potential energy surface.

The potential energy surface of CCl_4^- is given in Figure 2 as a contour map. The values are calculated as functions of r_1 and r_2 at the MP2/6-31G* level of theory. The other geometrical parameters are fixed to those of the neutral CCl_4. Figure 2 shows that two energy minima are bound on the PES, corresponding to the compressed and elongated structure. The elongated structure is strongly bound, whereas the energy minimum of the compressed one is very shallow. One expects that for a trajectory formed by vertical electron attachment in CCl_4 on the PES one will pass rapidly through a region of the compressed structure on the way to the elongated structure. This

TABLE 2: Total Energies and Relative Energies (ΔE) Calculated at the MP4SDQ/6-31G* Level

	species	total energy/au	ΔE/kcal mol^{-1}
CCl_4		−1876.4544	0.0
CCl_4^-	compressed	−1876.4483	3.8
	elongated	−1876.4672	−8.0
TS		−1876.4477	4.2
CCl_4^{-a}		−1876.4164	27.45
CCl_4^+	(=CCl_3^+ + Cl)	−1876.0732	(10.37 eV)
CCl_4^{+a}		−1876.0328	(11.47 eV)

[a] The energy with the geometry fixed in the neutral CCl_4 molecule.

TABLE 3: Optimized Parameters for CCl_4^+ Calculated at the MP4SDQ/6-31G* Level. Bond Lengths and Angles Are in Angstroms and Degrees

	CCl_4^+
r_1	10.10
r_2	1.6535
θ	89.92

feature of the trajectory, which will be confirmed by the trajectory calculations in the next section, is schematically illustrated as a dashed line in Figure 2.

B. Radical Cation CCl_4^+. The geometry optimization is carried out for CCl_4^+ at the MP4SDQ/6-31G* level of theory. However, the stable structure of CCl_4^+ was not obtained, but the dissociation products, i.e., CCl_3^+ and Cl, are obtained. This means that the radical cation of CCl_4^+ is unstable and spontaneously decomposed to CCl_3^+ and Cl by ionization of CCl_4. The optimized parameters for CCl_4^+ are given in Table 3. The vertical ionization potential of CCl_4 is calculated to be 11.5 eV. The energy of the vertical ionized CCl_4 with the neutral structure is 25.3 kcal/mol unstable relative to its dissociation limit (CCl_3^+ + Cl). This large energy difference implies that CCl_4^+, formed by vertical ionization of CCl_4, is rapidly dissociated to CCl_3^+ and Cl. This feature will also be confirmed by the following trajectory calculations.

II. Ab Initio Dynamics Trajectory Study. *A. Structure of Neutral CCl_4.* First, a trajectory of neutral CCl_4 is calculated in order to obtain the structure of CCl_4 at low temperature. The calculation was run for the constant temperature condition from the optimized structure of CCl_4. We chose 10 K for a simulation temperature and 0.01 ps for a bath relaxation time. The energy of the system was close to a constant value during simulation. The profile of the trajectory is given in Figure 3. Two bond distances are plotted as a function of time in Figure 3A. Both bond distances (r_1 and r_2) are oscillated in the range from 1.758 to 1.797 Å at 10 K. The Cl−C−Cl angle hardly fluctuated in the neutral system, as clearly seen in Figure 3B. These results indicate that the CCl_4 molecule has a very rigid structure at low temperature and has a small Franck−Condon (FC) region.

B. Electron Attachment Process in CCl_4. To elucidate the dynamics of CCl_4^- following vertical electron attachment, the ab initio trajectory calculations are carried out on the assumption of the vertical electron attachment in CCl_4. A total of 12 trajectories were run by using the initial structures randomly selected from the CCl_4 trajectory. All trajectory calculations gave the similar results. The potential energy for a sample trajectory is plotted in Figure 4 as a function of reaction time. The energy suddenly decreases and then increases in the short time region 0.0−0.08 ps. This energy lowering is due to the fact that the structure of CCl_4^- is rapidly deformed by the Jahn−Teller effect. After that, the energy gradually decreases. The C−Cl bond distances are plotted in Figure 4B (only two bond distances are given). All C−Cl bond distances in CCl_4^- are equivalent at time zero. At the short time region, one of the

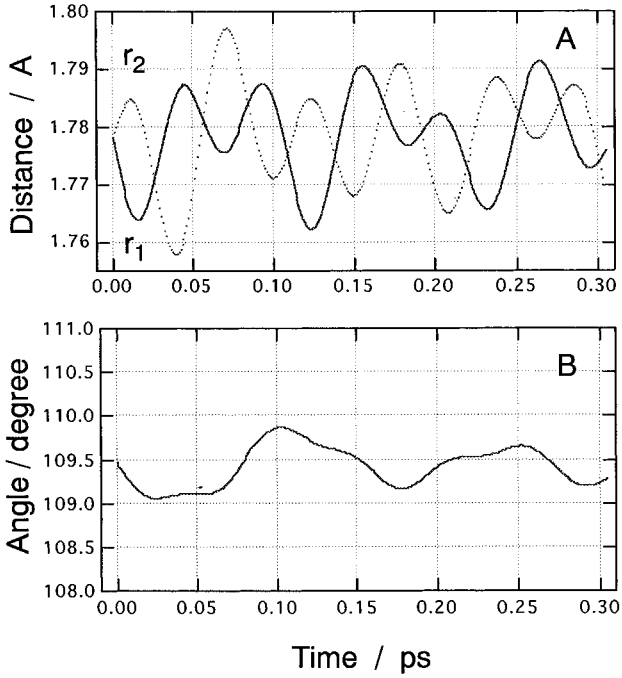

Figure 3. Trajectory for the neutral CCl_4 molecule plotted as a function of reaction time. The simulation is carried out at 10 K: (A) interatomic distances, r_1 and r_2, versus time and (B) bending angle θ versus time.

C−Cl bonds (denoted by r_2) is very elongated, whereas the other bond distances are slightly elongated and fluctuated around the equilibrium bond length. At a time region from 0.15 to 0.40 ps, one of the C−Cl bond distances becomes 3.5 Å due to the fact that excess energy distributes on the C−Cl stretching mode. In addition, the Cl−C−Cl angle fluctuates in the range 88−130°.

Snapshots of the structure as a function of time are illustrated in Figure 5 accompanied with the spin densities expressed by contour maps. At time zero, the structure is the same as that of the neutral CCl_4. The contour plot for the spin density implies that an unpaired electron is only localized on the central carbon atom, whereas the charge is spread over the molecule. After 0.20 ps where one of the C−Cl bonds is very elongated, the unpaired electron is occupied in the sp^3-hybrid orbital on the carbon atom. The negative charge is largest on the elongated Cl atom (−0.898). At 0.40 ps, the Cl atom is rebound at the turning point, and the electronic state of the Cl atom is close to the free Cl^- ion at this point. At 0.60 ps, the elongated atom is switched to the other Cl atom, so that the direction of the sp-spin−orbital on the central carbon atom is changed to the other Cl atom. These vibrational and bending mode excitations may be continued as long as the energy relaxation process is not considered. This process may be caused by collision with solvent molecules in the condensed phase.

C. Vertical Ionization Process in CCl_4. The vertical ionization process in the CCl_4 molecule was also investigated by means of the same procedure. The initial geometries of the CCl_4^+ are randomly selected from the trajectory of the neutral CCl_4 in the FC region. A total of 12 trajectories were run. All trajectories gave the dissociated product (i.e., CCl_3^+ and Cl atom). As a sample, the result for a trajectory started from the optimized structure is given in Figure 6. The energy of CCl_4^+ after hole capturing of CCl_4 suddenly decreases at a very short time period up to 0.1 ps. This energy lowering is −35.0 kcal/mol after 0.8 ps. After that, only the energy fluctuation caused by both C−Cl stretching and bending modes of the CCl_3 neutral radical is observed. The distance between the carbon and dissociating Cl atom is plotted in Figure 6C. The result implies

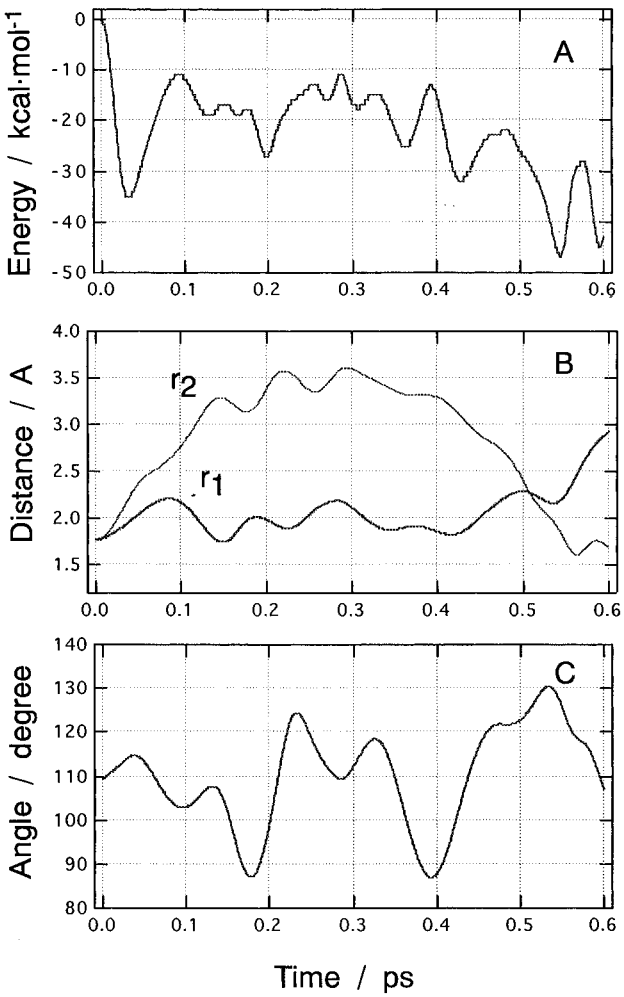

Figure 4. Sample trajectory for the CCl_4^- anion formed by the vertical electron attachment of CCl_4 plotted as a function of reaction time: (A) the potential energy of the reaction system, (B) interatomic distances, r_1 and r_2, and (C) bending angle θ versus time.

that a Cl atom dissociates from CCl_4^+, and the CCl_3^+ ion and Cl atom are formed within a very short time corresponding to one vibration period of the C−Cl stretching mode. Accompanied with the dissociation of the Cl atom, the bond distance of C−Cl in CCl_4^+ ion is shorten due to the fact that the C−Cl bond of CCl_3^+ is shorter than that of CCl_4. These results suggest that CCl_4^+ is spontaneously dissociated by capturing a hole.

Snapshots of the structure of CCl_4^+ for the sample trajectory after a vertical ionization of CCl_4 are illustrated in Figure 7. In addition, spin density and charge on each atom are given by contour maps and values, respectively. At time zero, an unpaired electron is mainly localized on one of the Cl atoms in CCl_4^+. The positive charge on the Cl atom (+0.777) is much larger than that of the other Cl atoms (+0.274, +0.254, and +0.273). After 0.1 ps where one of the C−Cl bonds is more elongated (3.45 Å), the unpaired electron is still localized on the dissociating Cl atom, although the charge is close to zero on the Cl atom. At a time of 0.2 ps, the system is composed of the dissociated product (CCl_3^+ ion and Cl atom), suggesting that the dissociation process is almost completed at 0.2 ps.

4. Discussion

In the present study, we treated two processes of CCl_4 by means of ab initio MO and ab initio dynamics calculations: these are the electron attachment and ionization processes in

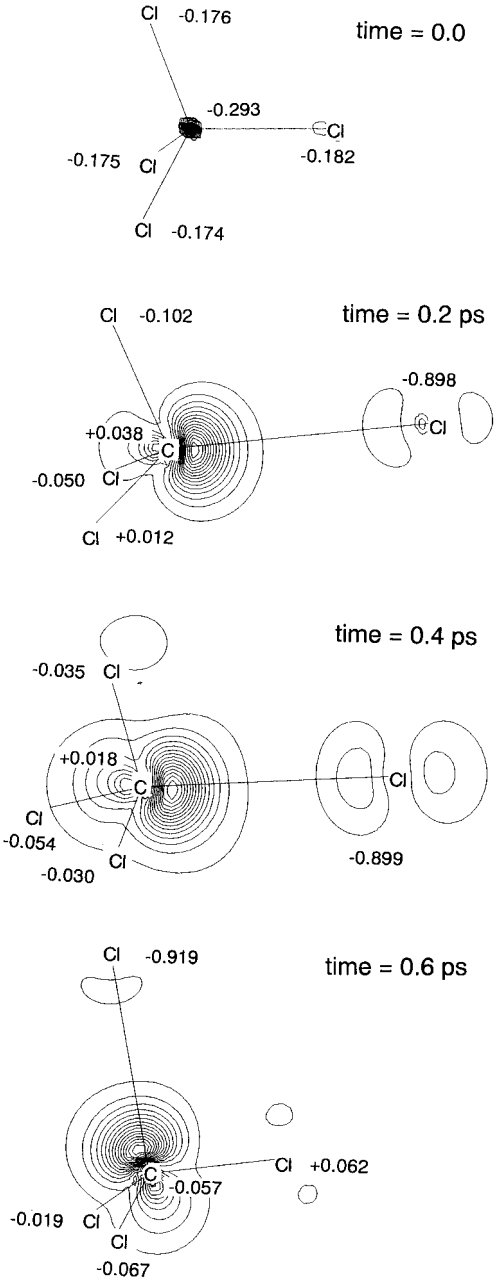

Figure 5. Snapshots for the CCl_4^- system as a function time. The contours and values indicate the spin densities and Mulliken charges on atoms calculated at the HF/3-21G* level.

CCl_4 (i.e, electron- and hole-capturing processes). On the basis of the present results, we would propose a reaction model for these processes. Potential energy curves expressed for electron attachment and ionization processes in CCl_4 are schematically illustrated in Figure 8A,B, respectively. Lower and upper curves in Figure 8 express the potential energies for the neutral and ionic species along the C−Cl bond, respectively. The upper curve in Figure 8A has two energy minima, corresponding to the elongated and compressed structures of CCl_4^-. Both structures are energetically lower than that of the dissociation limit ($CCl_3 + Cl^-$). The hatched region expresses that Franck−Condon (FC) region for a vertical electron attachment in CCl_4. The ab initio calculation indicated that the energy in the FC region on the PES of CCl_4^- is comparable to or slightly higher than that of the dissociation limit, suggesting that the dissociation of Cl^- from CCl_4^- may occur. However, the trajectory calculations rejected this proposition: the reaction energy distributes mainly to internal modes in CCl_4^-, so that the dissociation of CCl_4^- would be restricted by the dynamic effect

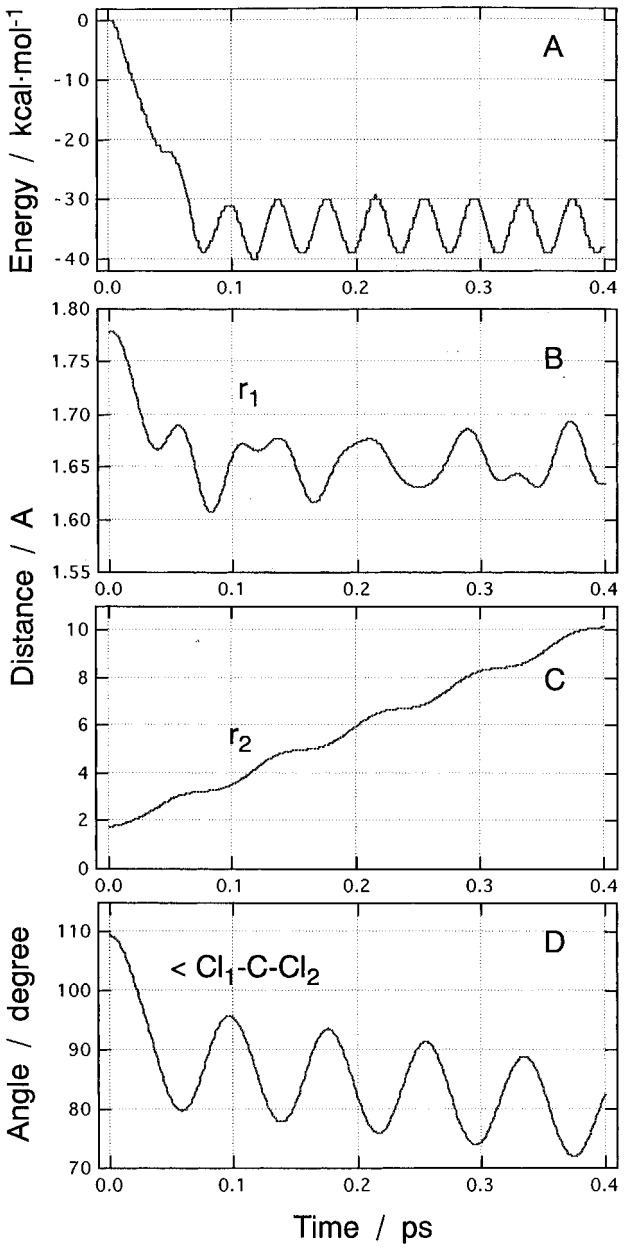

Figure 6. Sample trajectory for the CCl_4^+ formed by the vertical electron capturing of CCl_4 plotted as a function of reaction time: (A) the potential energy of the reaction system, (B) interatomic distances r_1 and (C) r_2, and (D) bending angle versus time.

in the case of zero excess energy of $[CCl_4^-]_{unstable}$. This feature is in qualitative agreement with the available experimental findings in the gas phase.[7,8]

Next, the medium effect on the structure of CCl_4^- is discussed because the experiments for the ionic species of CCl_4 are carried out mainly in the condensed phase.[3,4] Banazzola et al. measured the ESR spectra of CCl_4^- trapped in CCl_4 matrixes. They showed that CCl_4^- has axially symmetric *g*-tensors, indicating that the compressed and/or elongated structures contribute to the spectrum. From an analysis of hyperfine coupling constants (hfc's) of CCl_4^-, it was suggested that CCl_4^- is composed of three equivalent chlorines and one chlorine different from the others. The hfc of the latter one is as small as 25% of the former ones. The preliminary calculation of hfc's of CCl_4^- indicates that the compressed structure has one chlorine with a smaller hfc (17%) than the other ones.[14] In contrast, in the elongated structure the hfc of one of the chlorine atoms is 9 times larger than the other ones. This result strongly indicates that CCl_4^- exists as a compressed structure in CCl_4 matrixes at low

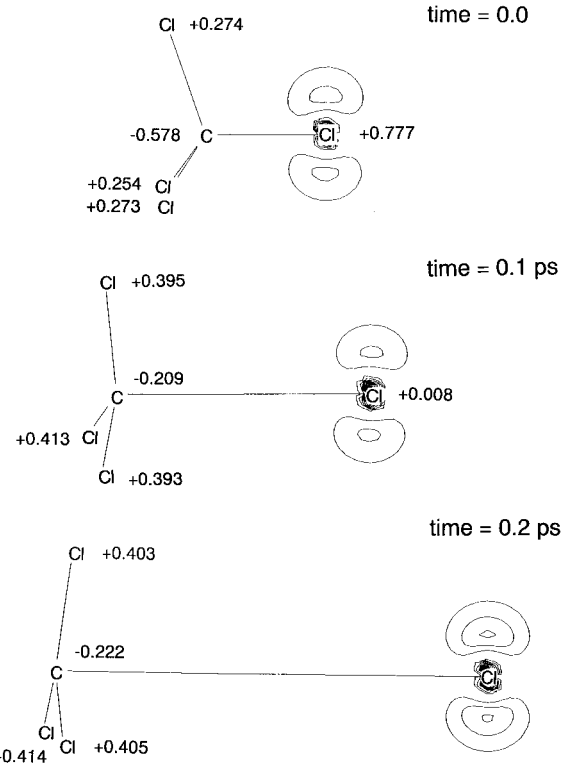

Figure 7. Snapshots for the CCl_4^+ system as a function of time. The contours and values indicate the spin densities and Mulliken charges on atoms calculated at the HF/3-21G* level.

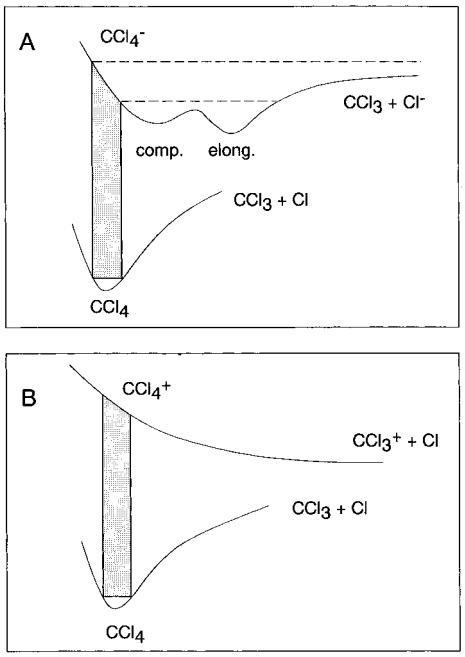

Figure 8. Reaction model for the electron (A) and hole (B) capturing processes in CCl_4. Lower and upper curves are potential energies for neutral and ionic species, respectively.

temperature. The excess energy of CCl_4^- after the vertical electron attachment of CCl_4 may disperse into the matrix molecule before the conversion from compressed to elongated structures, so that the compressed structure is dominant in the condensed phase.

The potential energy curves for the CCl_4^+ system are given in Figure 8B. The curve for the cationic system CCl_4^+ (upper curve) is strongly repulsive, and the energy of the FC region is always much higher than the dissociation limit. Hence there is no intermediate complex on the PES. This indicates that the

dynamics of CCl_4^+ is very simple and the CCl_4^+ dissociates rapidly to CCl_3^+ and Cl without excess energy. This feature in the CCl_4^+ is very similar to that of $CFCl_3^+$ reported by Lunell and co-workers.[2b]

We have introduced several approximations to calculate the potential energy surface and to treat the reaction dynamics. First, we assumed that the radical ions have no excess energy at the initial step of the trajectory calculation (time = 0.0 ps). This may cause a slight change of lifetime in the CCl_4^+ and of energy distribution in CCl_4^-. In the case of higher excess energy, the dissociation of Cl^- may occur in the CCl_4^- system. This effect was not considered in the present calculations. It should be noted therefore that the present model is limited in the case of no excess energy. Second, we assumed a HF/3-21G* multidimensional potential energy surface in the trajectory calculations throughout. A more accurate wave function may provide deeper insight into the dynamics. Despite the several assumptions introduced here, the results enable us to obtain valuable information on the mechanism of electron- and hole-capturing processes in CCl_4.

Acknowledgment. The author is indebted to the Computer Center at the Institute for Molecular Science (IMS) for the use of the computing facilities. The author acknowledges partial support from a Grant-in-Aid from the Ministry of Education, Science, Sports and Culture of Japan.

References and Notes

(1) Lund, A.; Shiotani, M. In *Radical Ionic Systems*; Lund, A., Ed.; Kluwer: Dordrecht, 1991.

(2) (a) Lunell, S.; Eriksson, L. A.; Fangstrom, T.; Maruani, J.; Sjoqvist, L.; Lund, A. *Chem. Phys*. **1993**, *171*, 119. (b) Huang, M.-B.; Lunell, S.; Karlsson, K. *Chem. Phys. Lett.* **1990**, *171*, 265. (c) Itagaki, Y.; Shiotani, M.; Tachikawa, H. *Acta Chim. Scand*. **1997**, *51*, 220.

(3) (a) Domazou, A. S.; Quadir, A. M.; Bühler, R. E. *J. Phys. Chem.* **1994**, *98*, 2877. (b) Bühler, R. E.; Hurni, B. *Helv. Chim. Acta* **1978**, *61*, 90.

(4) Bonazzola, L.; Michaut, J. P.; Roncin, J. *Chem. Phys. Lett.* **1988**, *153*, 52.

(5) (a) Gebicki, J. L.; Domazou, A. S.; Ha, T.-K.; Cirelli, G.; Bühler, R. E. *J. Phys. Chem*. **1994**, *98*, 9570. (b) Suwalski, J. P. *Radiat. Phys. Chem*. **1995**, *46*, 53. (c) Reed, A. E.; Weinhold, F.; Weiss, R.; Macheleid, J. *J. Phys. Chem.* **1985**, *89*, 2688.

(6) For example: (a) Bühler, R. E.; Ha, T.-K. *Radiat. Phys. Chem*. **1989**, *34*, 539. (b) Ichikawa, T.; Shiotani, M.; Ohta, N. *J. Phys. Chem*. **1989**, *93*, 4522. (c) Sumiyoshi, T., Sawamura, S.; Koshikawa, Y.; Katayama, M. *Bull. Chem. Soc. Jpn.* **1982**, *55*, 2341.

(7) Oster, T.; Kuhn, A.; Illenberger, E. *Int. J. Mass Spectrom. Ion Processes* **1989**, *89*, 1.

(8) *Electron-Molecule Interactions and Their Applications*; Christophorou, L. G., Ed.; Academic: New York, 1984.

(9) Gutsev, G. L. *J. Phys. Chem*. **1991**, *95*, 5773.

(10) (a) Tachikawa, H.; Ohnishi, K.; Hamabayashi, S.; Yoshida, H. *J. Phys. Chem.* **1997**, *101*, 2229. (b) Tachikawa, H. *J. Phys. Chem.* **1995**, *99*, 225. (c) Abe, M.; Inagaki, Y.; Springsteen, L. L.; Matsumi, Y.; Kawasaki, M.; Tachikawa, H. *J. Phys. Chem.* **1994**, *98*, 12641. (d) Tachikawa, H.; Hamabayashi, T.; Yoshida, H. *J. Phys. Chem.* **1995**, *99*, 16630. (e) Tachikawa, H.; Takamura, H.; Yoshida, H. *J. Phys. Chem.* **1994**, *98*, 5298. (f) Tachikawa, H.; Ohtake, A.; Yoshida, H. *J. Phys. Chem.* **1993**, *97*, 11944.

(11) (a) Tachikawa, H. *J. Phys. Chem.* **1996**, *100*, 17990. (b) Tachikawa, H.; Kumaguchi, K. *Int. J. Mass Spectrom. Ion Processes*, in press. (c) Ab initio MO calculation program: Frisch, M. J.; Trucks, G. W.; Schlegel, H. B.; Gill, P. M. W.; Johnson, B. G.; Robb, M. A.; Cheeseman; J. R.; Keith, T.; Petersson, G. A.; Montgomery, J. A.; Raghavachari, K.; Al-Laham, M. A.; Zakrzewski, V. G.; Ortiz, J. V.; Foresman, J. B.; Cioslowski, J.; Stefanov, B. B.; Nanayakkara, A.; Challacombe, M.; Peng, C. Y.; Ayala, P. Y.; Chen, W.; Wong, M. W.; Andres, J. L.; Replogle, E. S.; Gomperts, R.; Martin, R. L.; Fox, D. J.; Binkley, J. S.; Defrees, D. J.; Baker, J.; Stewart, J. P.; Head-Gordon, M.; Gonzalez, C.; Pople, J. A. *Gaussian 94*, Revision D.3; Gaussian, Inc.: Pittsburgh, PA, 1995.

(12) Granada, J. R.; Stanton, G. W.; Clarke, J. H.; Dore, J. C. *Mol. Phys*. **1979**, *37*, 1297.

(13) Burrow, P. W.; Modelli, A.; Chiu, N. S. *J. Chem. Phys*. **1982**, *77*, 2699.

(14) Tachikawa, H. Unpublished data.